

Submitted:
13.10.2025
Accepted:
09.02.2026
Published:
20.03.2026

Ultrasound imaging of small peripheral nerves – a primer for radiologists

Aakanksha Agarwal¹, Abhishek Chandra², Palak Dhakar¹, Mahesh Prakash³

¹ Department of Radiodiagnosis, Mahatma Gandhi Medical College and Hospital, Mahatma Gandhi University of Medical Sciences and Technology, Jaipur, India

² Department of Orthopedics, Mahatma Gandhi Medical College and Hospital, Mahatma Gandhi University of Medical Sciences and Technology, Jaipur, India

³ Departments of Radiodiagnosis and Imaging, Post Graduate Institute of Medical Education and Research, Chandigarh, India

Corresponding author: Mahesh Prakash; e-mail: image73@gmail.com

DOI: 10.15557/JoU.2026.0005

Keywords

ultrasound;
small nerve imaging;
high-frequency imaging

Abstract

High-resolution imaging has transformed the evaluation of small superficial peripheral nerves, enabling earlier detection of neuropathies, traumatic injuries, and entrapments. Among available modalities, ultrasound is particularly well suited for this purpose owing to its high spatial resolution, dynamic assessment capabilities, and ability to guide interventions. Normal nerves can be recognized on ultrasound by their fascicular architecture and characteristic honeycomb appearance, which helps distinguish them from adjacent tendons, vessels, and connective tissue. High-frequency transducers allow improved delineation of fascicular detail, while small-footprint probes enable imaging of nerves in anatomically constrained regions, establishing ultrasound as a reliable and cost-effective tool for evaluating peripheral nerve injuries. Because of spatial resolution limitations, magnetic resonance imaging has restricted ability to evaluate submillimeter-sized nerves; high-resolution ultrasound is therefore particularly effective in localizing pathological nerves – both in terms of the exact site of involvement and the length of the affected segment. This review article highlights in detail the sonographic techniques, pitfalls, and key anatomic landmarks for visualizing small peripheral nerves in the upper and lower extremities, with particular emphasis on nerves that are frequently under-evaluated in routine clinical practice yet often contribute to allodynia. Normal anatomical appearance on ultrasound is provided for better understanding along with examples of pathologies affecting these nerves.

Introduction

Peripheral nerves of the upper and lower extremity may be compromised by trauma, iatrogenic injury, repetitive strain, or neoplastic processes. Superficial nerves are particularly prone to injury by direct compressions and lacerations. They are also vulnerable to injury during graft harvesting and the creation of surgical entry portals. They may become entrapped at fascial exit sites due to repetitive strain or fascial injuries. While pathologies isolated to superficial nerves usually do not result in motor loss, as most small superficial nerves are sensory in nature, they can cause significant morbidity due to altered sensation within the affected dermatome and even anesthesia, which can lead to inadvertent injuries^(1,2).

Ultrasound is particularly useful in detecting early or subtle changes, even when electrodiagnostic evaluation shows no ab-

normality. On ultrasound, normal peripheral nerves are distinguished by their unique honeycomb echotexture, helping differentiate them from nearby tendons, vessels, and connective tissue^(3,4). Superficial nerves are best assessed using high-frequency (12–18 MHz) linear transducers that maximize spatial resolution. Ultra-high-frequency probes (e.g., 24-MHz) improve delineation of fascicular detail in superficial nerves. Small-footprint transducers, such as hockey-stick probes, facilitate assessment of nerve branches in anatomically constrained regions like the hand and wrist⁽²⁾.

Normal nerves on ultrasound show hypoechoic fascicles surrounded by an outer sheath of bright epineurium and echogenic perineurium enveloping the fascicles. In cross-section, this creates the classic honeycomb pattern that distinguishes nerves from adjacent tissues (Fig. 1).

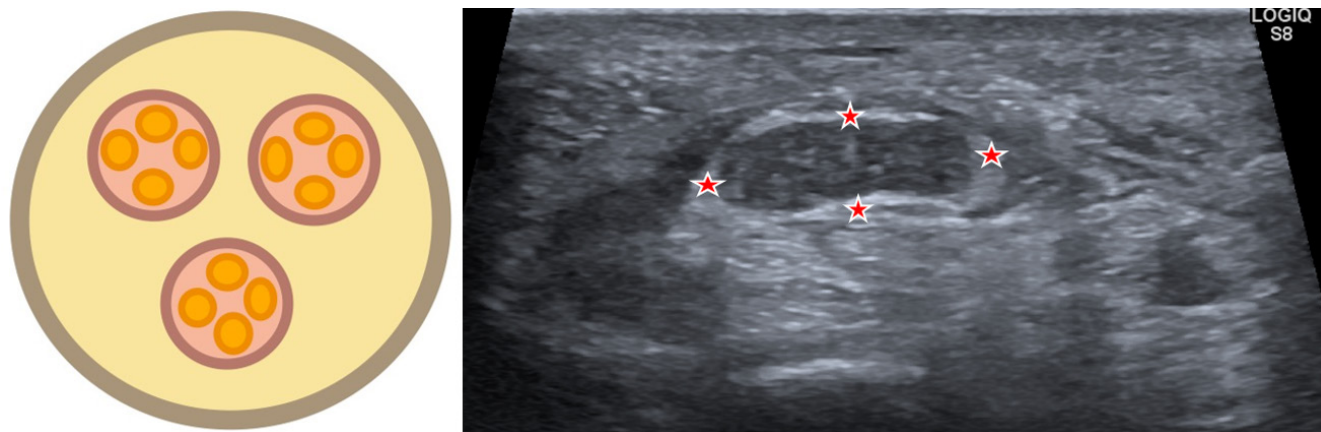


Fig. 1. Schematic diagram illustrating the honeycomb architecture of nerves when imaged in cross-section (yellow – epineurium; purple – perineurium; orange – endoneurium). The image on the right shows the normal honeycomb architecture of the median nerve (asterisk) with an echogenic epineurium

Nerves should first be traced in the short axis, with any abnormality subsequently assessed in the long axis, where their normal appearance includes parallel tubular fascicles separated by thin bright lines (Fig. 2).

Anisotropy is a common source of error in nerve ultrasound. Even slightly oblique insonation can make nerves appear falsely hypoechoic. Ensuring a perpendicular beam and comparing with the contralateral side improve diagnostic accuracy^(5,6).

Familiarity with sonographic landmarks, particularly osseous reference points, is essential for accurate identification of peripheral nerves and for procedural guidance.

In this review, we highlight the anatomic landmarks useful for evaluating less commonly assessed superficial peripheral nerves, focusing on the technical aspects of peripheral nerve ultrasound, common pitfalls, and detailed imaging strategies for small superficial nerves, with an emphasis on practical guidance for clinical application.

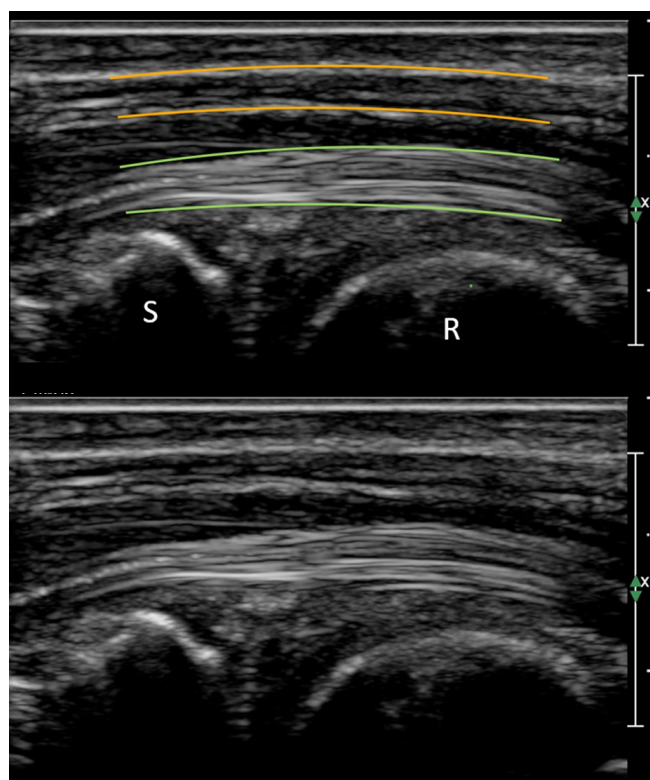


Fig. 2. Longitudinal image of the median nerve (yellow) and the underlying flexor tendon (green) within the carpal tunnel. The distal radius (R) and scaphoid (S) can be seen at inlet. Note the tubular appearance of the nerve, contrasting with the linear fascicular appearance of the underlying tendon

Medial antebrachial cutaneous nerve

High-resolution ultrasound consistently enables identification of the medial antebrachial cutaneous nerve in the mid-arm by exploiting its close proximity to the basilic vein. In a prospective study of healthy volunteers, the nerve was visualized adjacent to the vein in all participants, and ultrasound-guided blockade achieved a 100% success rate. This nerve, arising from the medial cord of the brachial plexus (C8–T1), courses within the brachial fascia alongside the basilic vein before branching toward the volar and ulnar aspects of the forearm. When scanned with a high-frequency transverse probe (≥ 15 MHz) and the patient supine with the arm abducted and externally rotated, the basilic vein serves as a reliable landmark, and Doppler imaging helps differentiate the fascicular nerve from vascular structures. This method is especially useful for diagnosing neuropathies following venipuncture or reconstructive surgery, and is also utilized for pre-operative nerve marking prior to elbow arthroscopy^(7–9) (Fig. 3).

Lateral antebrachial cutaneous nerve

The lateral antebrachial cutaneous nerve (LABCN), the terminal branch of the musculocutaneous nerve, is readily imaged with high-frequency sonography near the elbow crease. Positioned lateral to the biceps tendon and adjacent to the cephalic vein, the nerve can be visualized in the short-axis view. The cephalic vein, easily identified with minimal transducer pressure, serves as a landmark and helps trace the nerve’s origin from the musculocutaneous nerve within the biceps muscle using a linear probe (15–18 MHz) with the patient supine and the elbow slightly flexed. With the probe placed at the

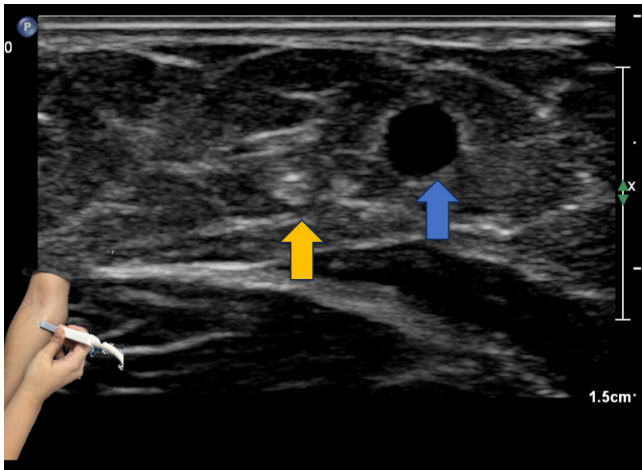


Fig. 3. The medial antebrachial cutaneous nerve (yellow arrow) can be identified adjacent to the basilic vein (blue) within the subcutaneous fat, superficial to the muscular fascia. The probe position is shown in the inset image. Care should be taken to ensure minimal probe pressure to identify the basilic vein

elbow crease, the biceps tendon is seen centrally and the brachial artery medially. The LABCN lies lateral to the biceps tendon, then courses subcutaneously along the radial aspect of the forearm⁽¹⁰⁾ (Fig. 4).

Injuries most frequently arise from venipuncture or distal biceps tendon tears. Sonographically, the nerve may appear enlarged or hypoechoic with altered echotexture. Dynamic imaging during forearm rotation (supination/pronation) can reveal entrapment by tendon during movement (Fig. 4).

Superficial branch of the radial nerve

Ultrasound reliably delineates the superficial branch of the radial nerve (SBRN), making it particularly useful in diagnosing Wartenberg's syndrome – an entrapment neuropathy at the distal forearm and wrist. Anatomically, the SBRN emerges beneath the brachioradialis tendon and lies adjacent to the cephalic vein, both of which serve as important sonographic landmarks. The nerve can be traced from its origin in the proximal forearm as it courses radially and distally, where

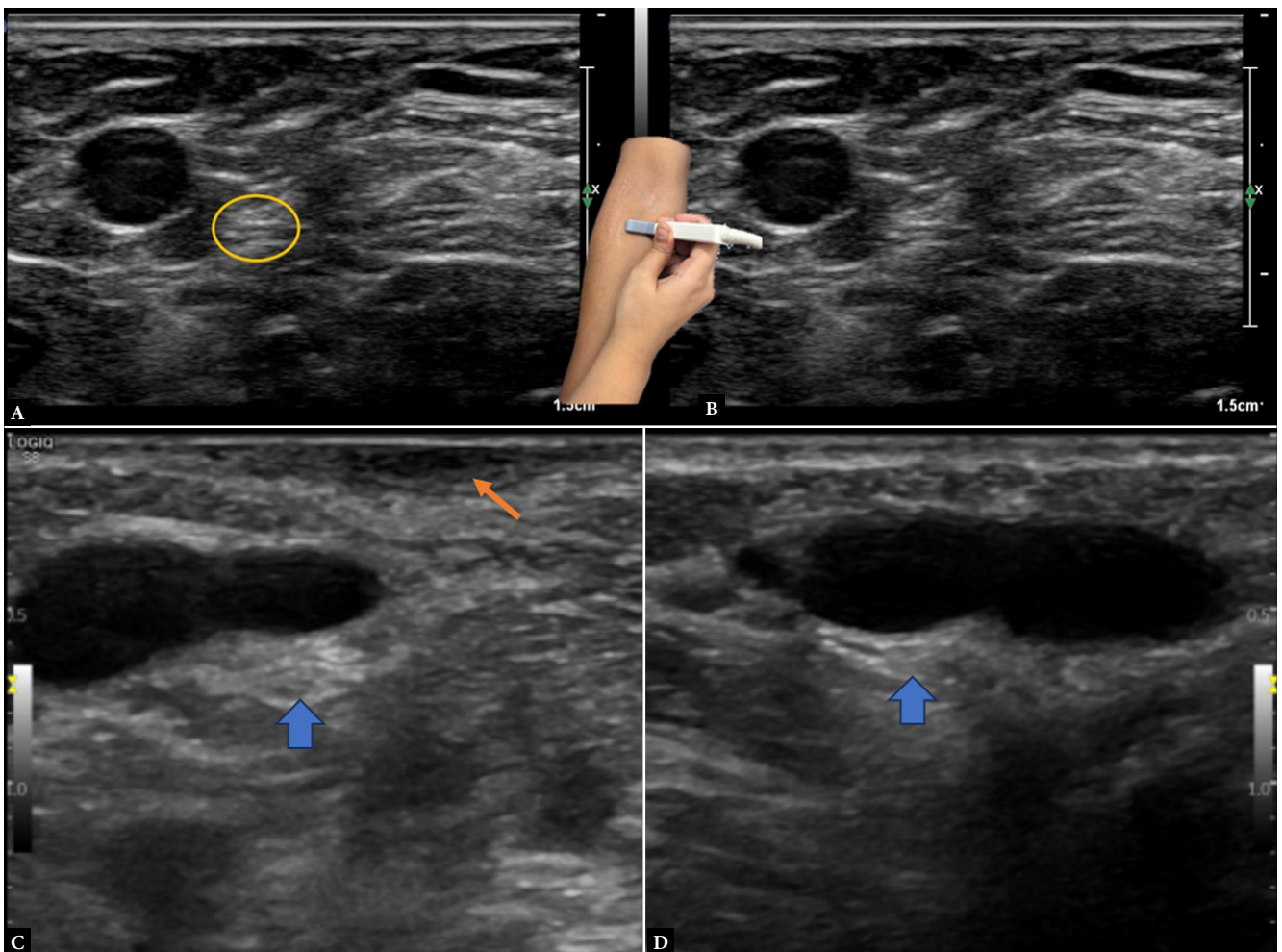


Fig. 4. The lateral antebrachial cutaneous nerve (yellow circle) is identified in the antecubital fossa, adjacent to the cephalic vein (A and B). Note probe position in the inset. Image C demonstrates thickening of the LABCN (blue arrow) in a patient following biceps tendon repair, compared to the contralateral normal nerve in image D. The orange arrow demonstrates focal scarring of the overlying skin in image C, indicating prior surgical intervention

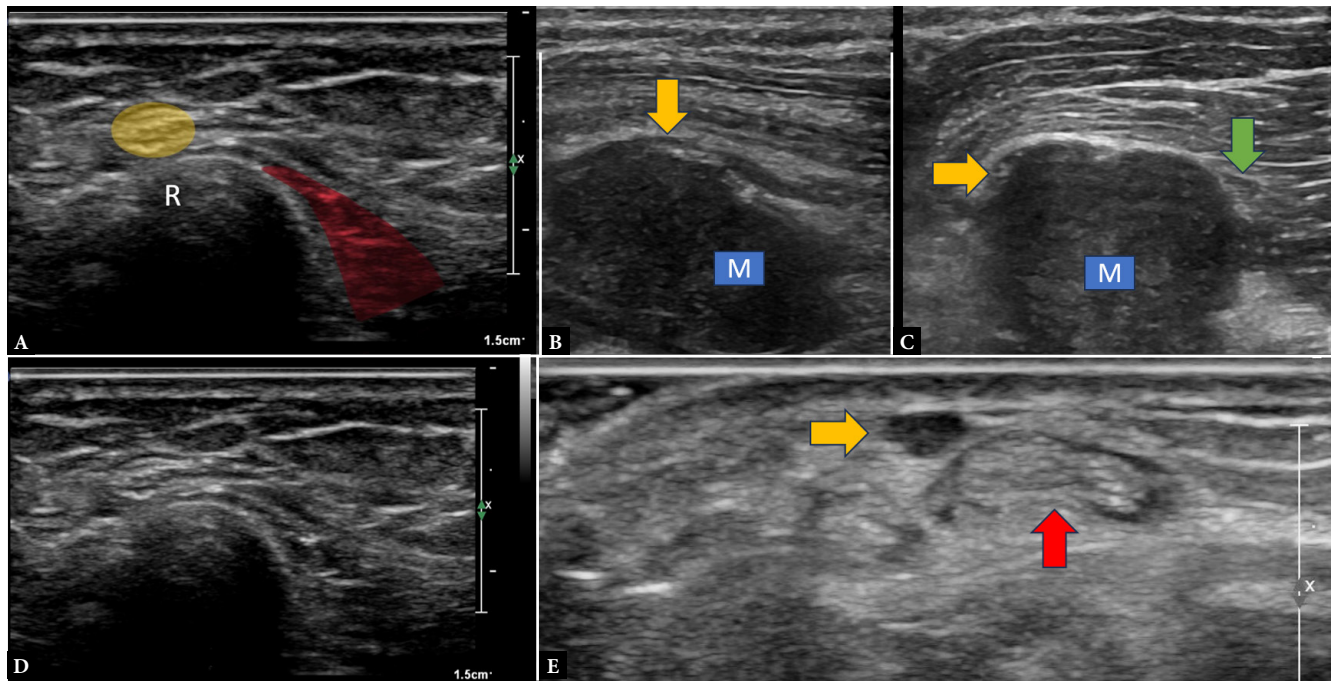


Fig. 5. Images A and B demonstrate the normal superficial branch of the radial nerve (yellow) in the distal forearm as it travels in the subcutaneous plane, curving over the distal radius (R) and lying superficial and lateral to the distal brachioradialis muscle (red). Images C and D demonstrate a hypoechoic mass lesion (M) closely abutting the SBRN (yellow arrow) and the posterior interosseous nerve (green arrow) just distal to their origin from the radial nerve in the proximal forearm. Image E demonstrates focal thickening of the SBRN (yellow arrow) at the level of the wrist, superficial to the first extensor compartment tendons (red arrow), which show mild effusion consistent with DeQuervain's tenosynovitis

it can be seen emerging from under the brachioradialis. It then travels in the subcutaneous plane after piercing the muscular fascia and continues distally toward the thumb. At this level, it wraps over the first extensor compartment, a common site of entrapment or iatrogenic injury associated with injections for DeQuervain's tenosynovitis^(11,12) (Fig. 5).

Dorsal branch of the ulnar nerve

The dorsal cutaneous branch of the ulnar nerve (DCBUN) is a terminal branch that arises from the ulnar nerve in the distal forearm. It passes volar to the ulna and dorsal to the flexor carpi ulnaris tendon before piercing the antebrachial fascia to become subcutaneous. From there, the nerve courses superficially along the dorsoulnar aspect of the hand and provides sensory supply to the dorsum of the fifth finger, the dorsoulnar portion of the fourth finger, and adjacent hand regions. Injuries to the DCBUN may be traumatic or iatrogenic. The nerve is particularly at risk during surgical approaches to the subcutaneous border of the ulna, such as those employed for open reduction and internal fixation of ulnar fractures. Sonographically, it can be identified in the distal forearm as it arises from the ulnar nerve in close association with the flexor carpi ulnaris⁽¹³⁾ (Fig. 6).

Palmar cutaneous branch of the median nerve

Sonographic identification of the palmar cutaneous branch of the median nerve (PCBmn) is both feasible and clinically valuable. In one study using 17–5 MHz probes, the PCBmn was visualized from its origin to slightly distal to the wrist crease in 83%

of healthy volunteers; in symptomatic individuals, abnormalities such as focal swelling, neuroma, or transection were detected in 55% of cases. Another sonographic study detailed its course: it emerges radially from the median nerve, pierces the antebrachial fascia between the flexor carpi radialis and palmaris longus tendons, and then travels superficial to the abductor pollicis brevis muscle (Fig. 7).

Extensive anatomical variation exists in the PCBmn, with the nerve piercing the antebrachial fascia at variable distances from the wrist crease, sometimes coursing through the carpal tunnel, travelling within the sheath or even within the substance of the flexor carpi radialis tendon; less commonly, it is associated with the palmaris longus. Awareness of these variants is essential to avoid iatrogenic injury during carpal tunnel release and to guide postoperative evaluation of persistent pain, which usually presents as 'pillar pain'^(14–16).

Digital nerves of hand

Digital nerve injury is a frequent consequence of penetrating trauma or surgical laceration, and sonography can detect discontinuity, neuroma formation, or focal thickening. Using high-frequency probes, paired neurovascular bundles can be identified adjacent to the flexor tendons with minimal transducer pressure. Scanning is initiated at the volar base of the finger along the flexor tendon sheaths, lateral to the digital arteries, and the neurovascular bundles are then followed distally alongside the tendons. The standoff pad or generous application of gel helps maintain acoustic coupling while avoiding excessive pressure, particularly when evaluating digital nerves near the fingertips^(17,18) (Fig. 8).

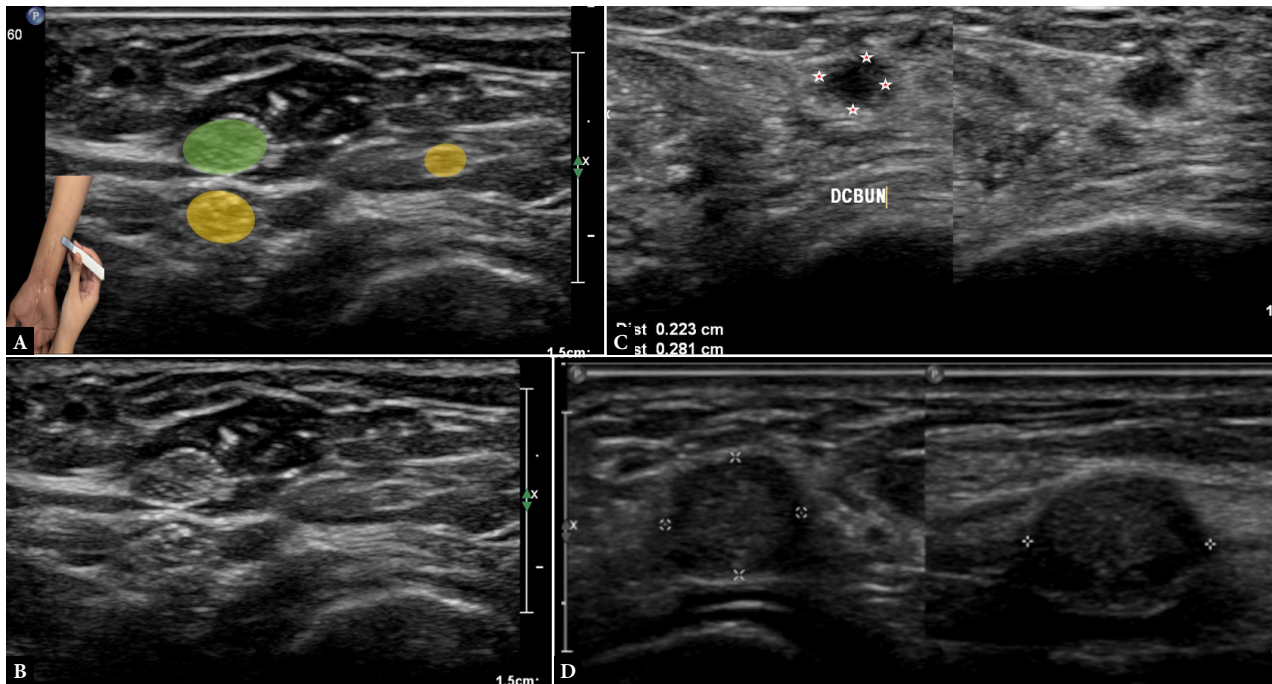


Fig. 6. Images A and B demonstrate the normal dorsal cutaneous branch of the ulnar nerve (smaller yellow circle) arising from the ulnar nerve (yellow circle) in the distal forearm (inset). The ulnar nerve lies deep to the flexor carpi ulnaris tendon (red) and gives rise to the DCBUN, which wraps over the ulna and travels in the subcutaneous plane of the dorsal forearm. Image C demonstrates neuroma formation within the DCBUN (asterisk) in a patient with a glass-cut injury in the distal forearm. Image D shows a hypoechoic mass along the DCBUN (asterisk) in the distal dorsal forearm in orthogonal planes, consistent with a peripheral nerve sheath tumor, presenting as a hypoechoic fusiform lesion with the DCBUN seen as a tail at both ends

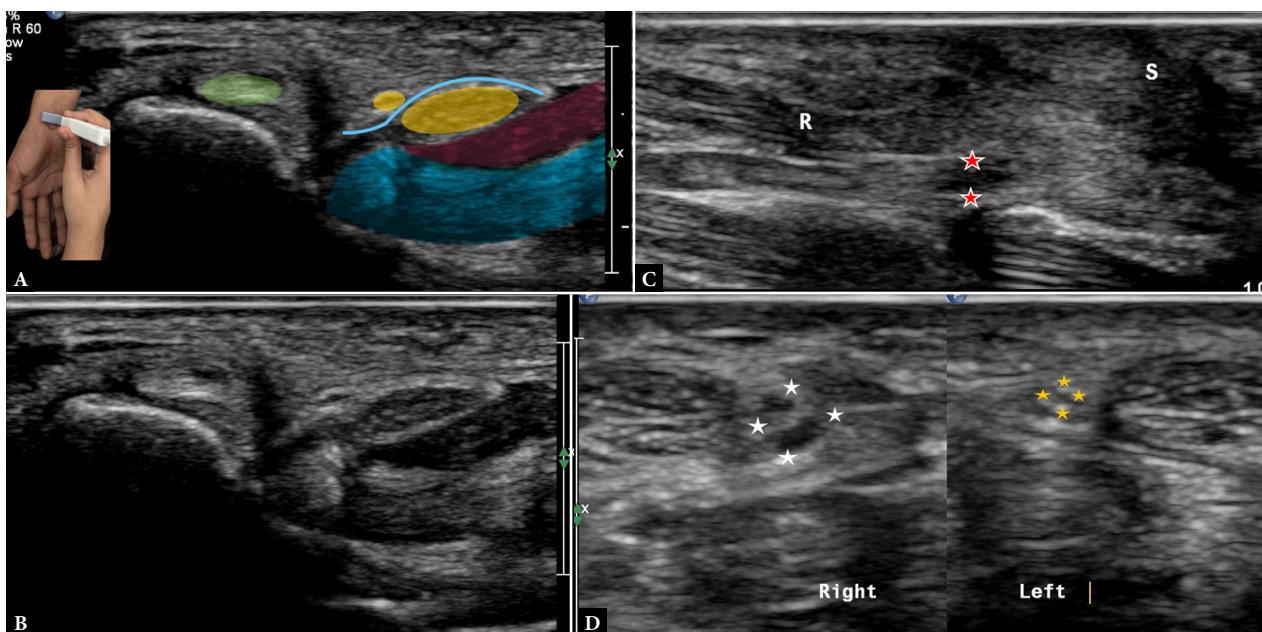


Fig. 7. Images A and B demonstrate one of the variant anatomical courses of the palmar cutaneous branch of the median nerve (PCBmn) (small yellow circle). Here, the nerve can be seen ulnar to the flexor carpi radialis (green circle) and superficial to the flexor retinaculum (blue) at the level of the carpal tunnel. In this patient, the nerve courses in the subcutaneous plane more distally than usual. Note the probe position in the inset. The median nerve (yellow circle), flexor tendons (blue), and an incidental low-lying muscle belly of flexor tendons (red) can also be seen. Image C shows an end-neuroma (asterisk) in the PCBmn in a patient with a penetrating injury in the distal forearm. The flexor carpi radialis (R) lies superficial to the nerve, and overlying hypoechoic scar (S) is also present. Image D demonstrates focal thickening of the PCBmn (white asterisk) as it courses medial to the flexor carpi radialis tendon in a patient with thenar pain. This can be compared with the contralateral normal side (yellow asterisk). The median nerve was normal in course and caliber in this patient

Lateral femoral cutaneous nerve

The lateral femoral cutaneous nerve (LFCN), a purely sensory branch of the lumbar plexus, emerges from the lateral border of the psoas major, crosses the iliacus, and usually passes beneath the inguinal ligament near the anterior superior iliac spine (ASIS). Its variable course makes ultrasound an ideal modality for localization. With the patient supine, a high-frequency linear probe is placed transversely at the ASIS. The nerve is typically seen between the sartorius and tensor fasciae lata muscles, appearing as a small hypoechoic fascicular structure superficial to the muscular fascia, and it can be traced proximally toward the inguinal ligament. Sonographic identification is particularly useful in meralgia paresthetica, where the nerve may appear thickened or hypoechoic at the site of entrapment, usually as it courses under the inguinal ligament at the groin crease. Ultrasound also improves the accuracy of targeted perineural injections⁽¹⁹⁻²¹⁾ (Fig. 9).

Medial femoral cutaneous nerve

The medial femoral cutaneous nerve, a branch of the femoral nerve, supplies the medial thigh and anterior knee. Its close relationship to

the sartorius muscle and the great saphenous vein provides reliable landmarks for sonographic identification. Although small, the nerve can be visualized with high-resolution ultrasound as a hypoechoic fascicular structure coursing within the superficial fascia along the medial thigh. Clinically, it is vulnerable to iatrogenic injury during medial thigh surgery or saphenous vein harvesting, and ultrasound is increasingly employed to evaluate unexplained medial thigh pain or sensory deficits in postoperative patients⁽²⁰⁾ (Fig. 10).

Saphenous nerve

The saphenous nerve courses along the medial aspect of the thigh, positioned lateral to the femoral vessels, and passes through the adductor canal beneath the sartorius muscle. In the lower half of the canal, it lies deep to the vastoadductor membrane, while the nerve to the vastus medialis remains superficial. Distally, thickening of the vastoadductor membrane represents a potential site for nerve entrapment. The saphenous nerve gives rise to the infrapatellar branch in the lower thigh, immediately distal to the adductor hiatus. Following the origin of the infrapatellar branch, the main trunk accompanies the saphenous branch of the descending genicular artery

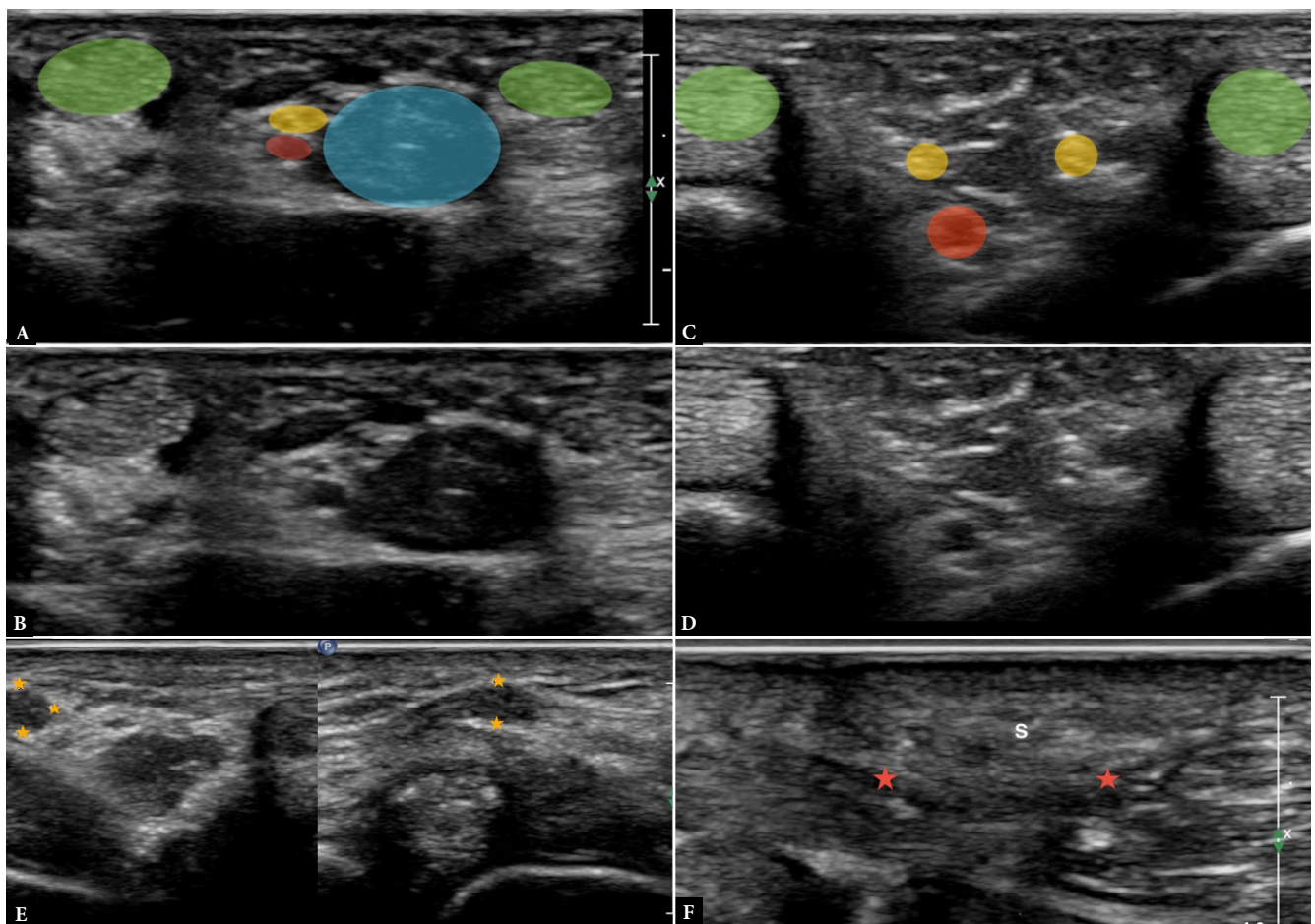


Fig. 8. Images A and B demonstrate the common digital nerve (yellow circle) at the level of the metacarpal head, with the lumbrical muscle (blue) between the flexor tendons (green). The red circle marks the digital vessels. Images C and D show the ulnar and radial branches of the digital nerve (yellow circle) as they course along adjacent fingers. The flexor tendons of the respective fingers can also be seen (green). Image E demonstrates a neuroma in two orthogonal planes in continuity with a common digital nerve (asterisk). Image F shows entrapment of the ulnar digital nerve (red asterisk) of the thumb within scar tissue (S) in a patient following pulley release

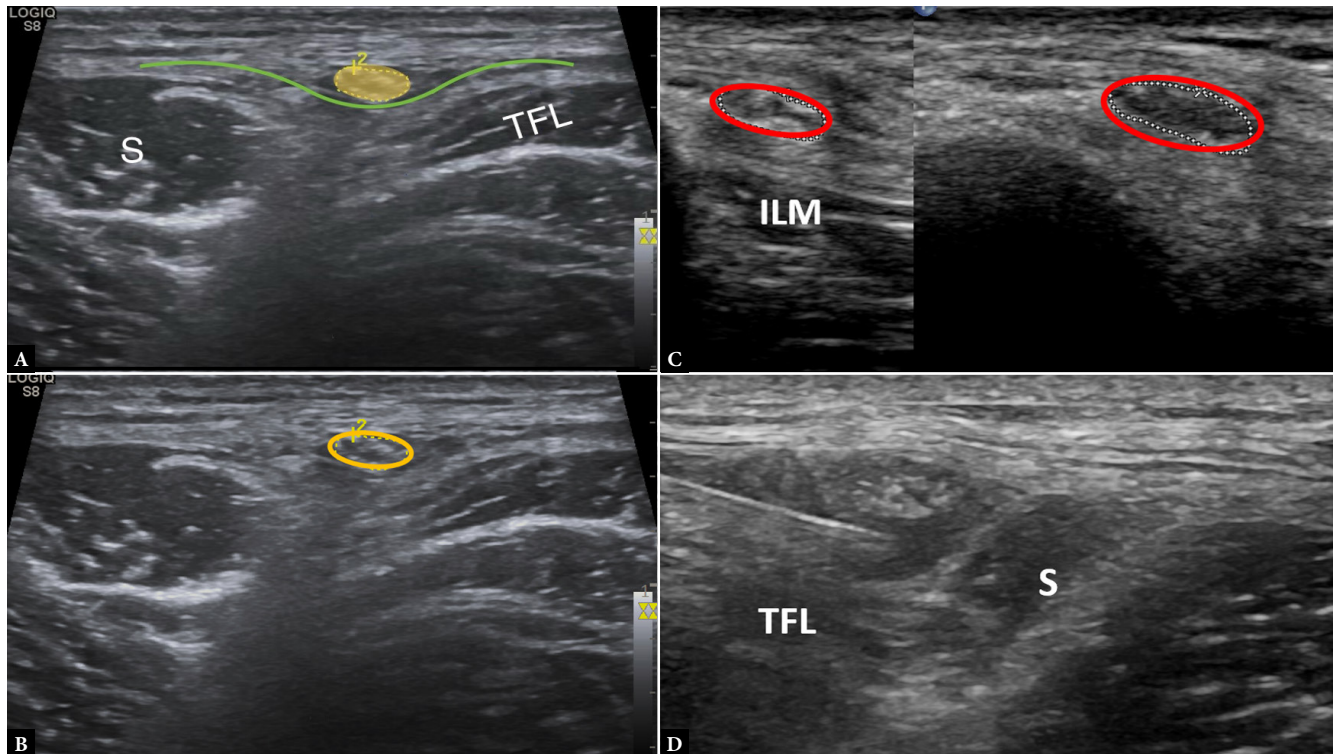


Fig. 9. Images A and B demonstrate the lateral femoral cutaneous nerve (yellow circle) superficial to the muscular fascia (green), lying between the sartorius (S) anteriorly and the tensor fasciae latae (TFL) posteriorly. Image C shows thickening of the LFCN as it crosses the inguinal ligament (encircled). The normal proximal caliber of the LFCN can be seen at the level of the iliacus muscle (ILM). Image D demonstrates ultrasound-guided perineural hydrodissection of the LFCN as it courses superficial to the muscular fascia between the TFL and sartorius

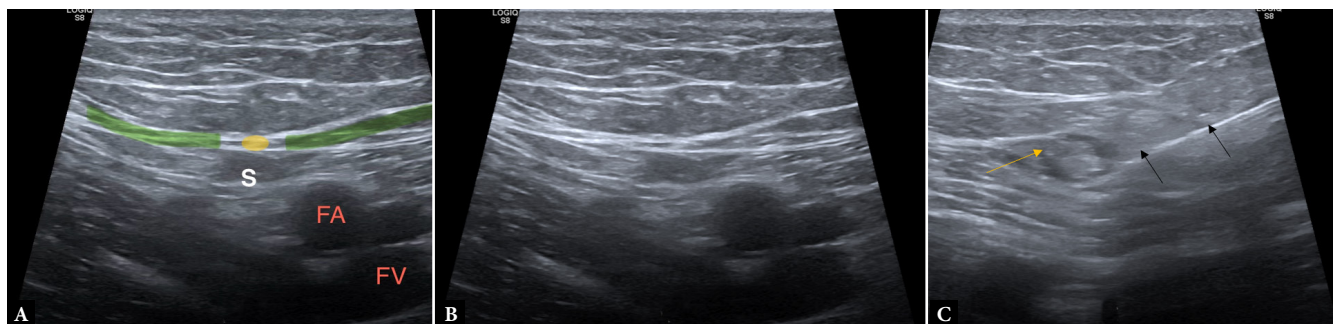


Fig. 10. Images A and B demonstrate the normal medial femoral cutaneous nerve superficial to the femoral vascular bundle, distal to the femoral canal. The nerve originates from the femoral nerve and travels medially, piercing the muscular fascia (green) over the sartorius (S) to innervate the medial thigh. Image C shows a perineural steroid injection around the medial femoral cutaneous nerve within the subcutaneous plane, superficial to the sartorius, in a diabetic patient with persistent pain along the distribution of this nerve

along the medial aspect of the leg. At a variable level, it pierces the crural fascia to enter the subcutaneous plane, where it lies in close association with the great saphenous vein^(2,20) (Fig. 11).

Sural nerve

The sural nerve, formed by contributions from the tibial and common peroneal nerves, runs with the small saphenous vein along the posterior calf and ankle. The lateral sural nerve arises at the level of the popliteal fossa from the common peroneal nerve, proximal to the fibular head. Ultrasound reliably demonstrates the sural nerve as a hypoechoic fascicular structure lateral to the

Achilles tendon in the lower leg, and it can be traced proximally from this site as it lies superficial to the gastrocnemius muscle bellies. Because of its superficial location, the sural nerve is prone to iatrogenic injuries in procedures around the ankle, and pre-procedural sonographic mapping can help reduce such complications⁽²⁰⁾ (Fig. 12).

Superficial peroneal nerve

The superficial peroneal nerve arises from the common peroneal nerve, becoming superficial in the distal third of the leg before dividing into dorsal cutaneous branches. It is visualized as it emerges

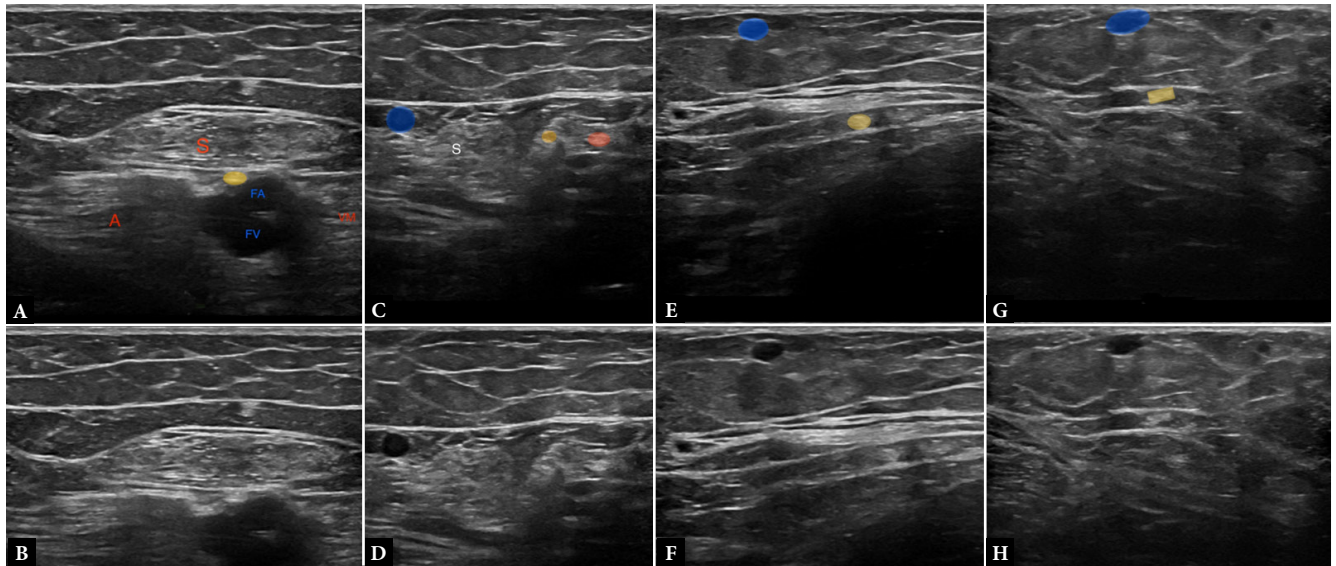


Fig. 11. Images A and B demonstrate the normal saphenous nerve (yellow) within the adductor canal, deep to the sartorius (S) and the vastoadductor membrane between the vastus medialis (VM) and adductor magnus (A). Images C and D show the saphenous nerve (yellow) after piercing the vastoadductor membrane and giving rise to the infrapatellar branch (green). Note its proximity to the great saphenous vein (blue). Images E and F demonstrate the saphenous nerve (yellow) in the lower medial thigh before piercing the medial muscular septum. In images G and H, the nerve (yellow) lies in the subcutaneous plane in close relation to the great saphenous vein (blue)

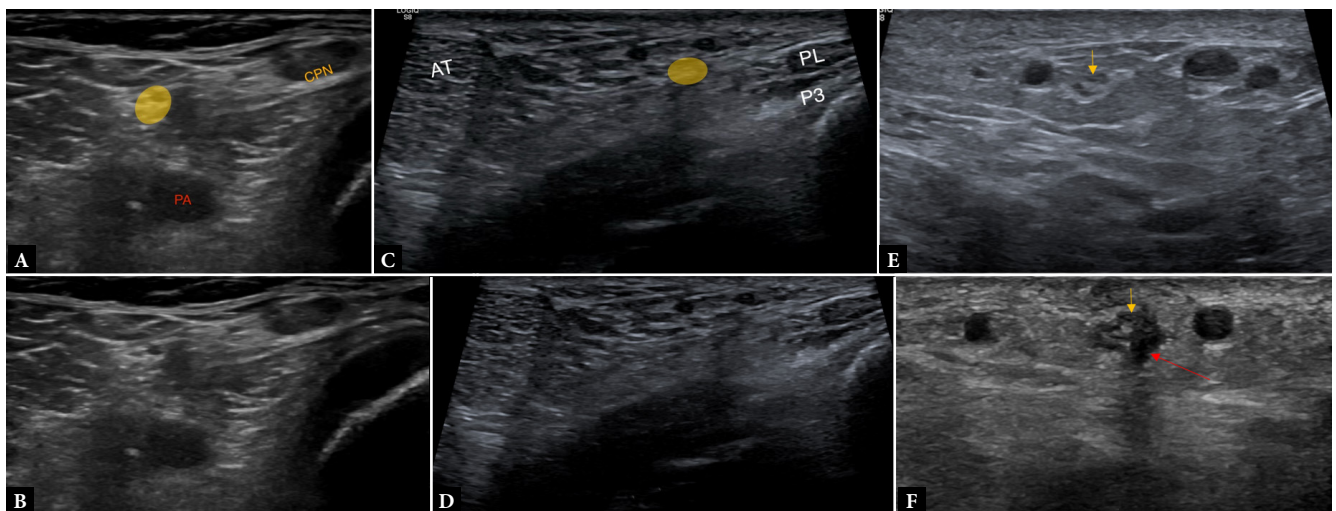


Fig. 12. Images A and B demonstrate the origin of the sural nerve (yellow) in the lateral aspect of the popliteal fossa from the common peroneal nerve (CPN). Here, the CPN is thickened, while the sural nerve remains normal in caliber and echogenicity. Images C and D demonstrate the sural nerve (yellow) at the level of the lateral ankle within the subcutaneous plane between the Achilles tendon (AT) and the peroneal tendons (PL/PB). Image E demonstrates edema within the sural nerve (yellow arrow) in the distal leg, and image F demonstrates a partial neuroma in the sural nerve (yellow arrow) at the level of the ankle following arthroscopy. The red arrow demonstrates the portal site and route, coursing along the lateral margin of the nerve, resulting in partial epineurial disruption

between the peroneus longus and brevis muscles and pierces the crural fascia. Variations in the fascial exit point are common and may predispose to entrapment neuropathy, particularly in athletes and patients with chronic ankle instability. Ultrasound is valuable both for diagnosis – demonstrating focal nerve enlargement or hypoechoogenicity at the fascial penetration site – and for guiding therapeutic hydrodissection or perineural injections^(2,22-24) (Fig. 13).

Intermetatarsal nerve

The intermetatarsal nerves, commonly discussed in the context of Morton’s neuroma, are another group of small peripheral nerves best evaluated with high-resolution sonography. These nerves course along the plantar aspect of the forefoot, between the metatarsal heads, superficial to the interosseous muscles and deep to the transverse metatarsal ligament⁽²⁵⁾. In healthy individuals, they

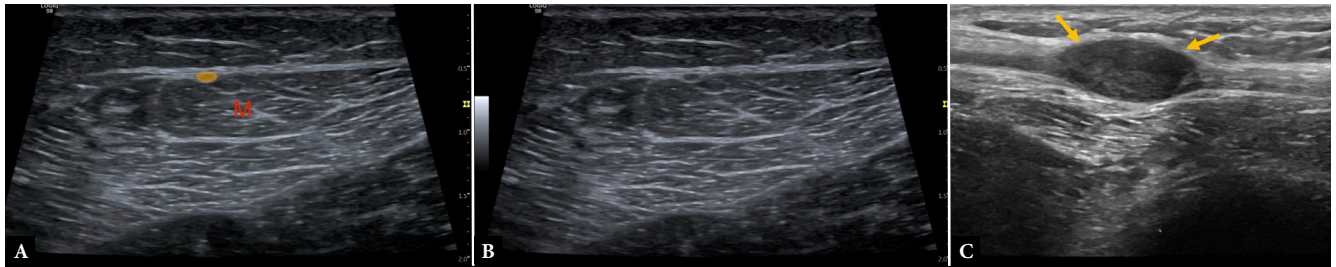


Fig. 13. Images A and B demonstrate the normal superficial peroneal nerve (yellow) in the mid-lower leg as it pierces the lateral muscular septum, with underlying lateral muscle bellies (M). Image C shows a peripheral nerve sheath tumor involving the superficial peroneal nerve (arrows)

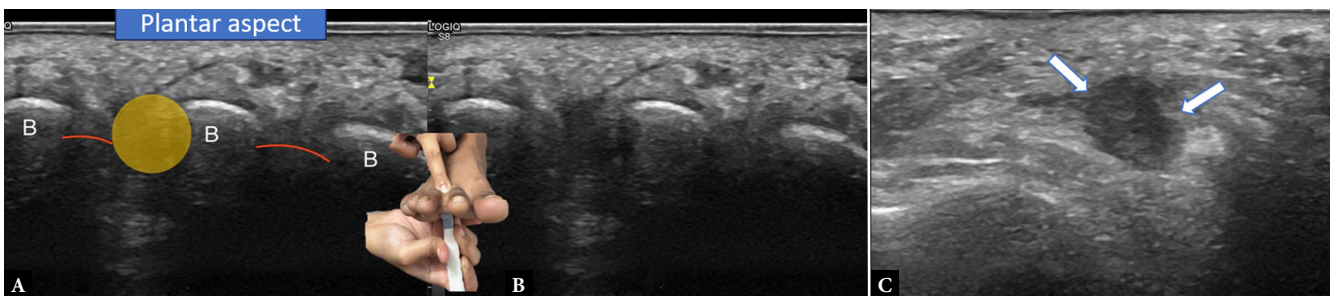


Fig. 14. Images A and B show an intermetatarsal neuroma (yellow) imaged from the plantar aspect with the probe placed transversely at the level of the metatarsal heads. The metatarsal heads (B) and the intermetatarsal ligament (red) can be seen. Finger pressure from the dorsal aspect accentuates the appearance of the neuroma by displacing it superficially. Image C shows the neuroma (between arrows) in the longitudinal plane

appear as thin, hypoechoic, fascicular structures; however, when thickened or compressed, they may form fusiform enlargements classically described as Morton’s neuroma. Ultrasound has been shown to be highly sensitive in identifying these neuromas, with diagnostic accuracy comparable to MRI⁽²⁶⁾. A dynamic technique, applying forefoot compression, may accentuate bulging between the metatarsal heads. This is performed by placing the probe longitudinally in the intermetatarsal space on the plantar aspect and using a finger to compress the tissues from the dorsal aspect with an aim to accentuate bulging deep to the transverse metatarsal ligament⁽²⁾. Ultrasound not only facilitates diagnosis but also guides therapeutic interventions such as corticosteroid or alcohol injections, allowing real-time confirmation of accurate perineural injectate placement⁽²⁷⁾ (Fig. 14).

Conclusion

Injuries and pathologies of small peripheral nerves are relatively common, primarily due to their superficial location, which predisposes them to trauma, iatrogenic injury, and entrapment at fascial exit sites just before they course into the subcutaneous plane. Pathologies of superficial nerves often result in significant pain and

functional impairment, underscoring the importance of early recognition and intervention. This pictorial review provides a comprehensive overview of the superficial nerves of the upper and lower extremities, highlighting key anatomical landmarks, sonographic identification techniques, and the spectrum of associated pathological conditions. The expanding role of ultrasound in the evaluation and management of these nerves offers a valuable opportunity to optimize patient care through accurate diagnosis and a range of minimally invasive treatment options.

Conflict of interest

The authors do not report any financial or personal connections with other persons or organizations which might negatively affect the contents of this publication and/or claim authorship rights to this publication.

Author contributions

Original concept of study: AA, MP. Writing of manuscript: AA, PD. Analysis and interpretation of data: AA, PD. Collection, recording and/or compilation of data: AA, AC. Critical review of manuscript: MP.

References

- Hannaford A, Vucic S, Kiernan MC, Simon NG. Review article "Spotlight on ultrasonography in the diagnosis of peripheral nerve disease: the evidence to date". *Int J Gen Med*. 2021 Aug 16;14:4579–4604. doi: 10.2147/IJGM.S295851.
- Agarwal A, Chandra A, Shirodkar K, Shah A, Murray TE, Iyengar KP, et al. "Small but mighty" – a radiologists' primer for ultrasound imaging of the smaller peripheral nerves. *Skeletal Radiol*. 2025 Jul;54(7):1373–1390. doi: 10.1007/s00256-024-04844-8.
- Chang KV, Mezian K, Naňka O, Wu WT, Lou YM, Wang JC, et al. Ultrasound Imaging for the cutaneous nerves of the extremities and relevant entrapment syndromes: from anatomy to clinical implications. *J Clin Med*. 2018 Nov 21;7(11):457. doi: 10.3390/jcm7110457.
- Vlassakov KV, Sala-Blanch X. Ultrasound of the peripheral nerves. In: Tubbs RS, Rizk E, Shoja MM, Loukas M, Barbaro N, Spinner RJ, editors. *Nerves and nerve injuries* [Internet]. Philadelphia: Elsevier; 2015 [cited 2025 Dec 15]. p. 227–250. Available from: <https://linkinghub.elsevier.com/retrieve/pii/B9780124103900000172>.
- Boehm J, Scheidl E, Bereczki D, Schelle T, Arányi Z. High-resolution ultrasonography of peripheral nerves: measurements on 14 nerve segments in 56 healthy subjects and reliability assessments. *Ultraschall Med*. 2014 Oct;35(5):459–467. doi: 10.1055/s-0033-1356385.
- Kasehagen B, Ellis R, Pope R, Russell N, Hing W. Assessing the reliability of ultrasound imaging to examine peripheral nerve excursion: a systematic literature review. *Ultrasound Med Biol*. 2018 Jan;44(1):1–13. doi: 10.1016/j.ultrasmedbio.2017.08.1886.
- Al-Qattan MM, Thallaj AK. High-resolution ultrasound as an aid in the diagnosis and treatment of post-brachio-plexus injury to the medial brachial and the medial antebrachial nerves – Two case reports. *Int J Surg Case Rep*. 2020;72:520–523. doi: 10.1016/j.ijscr.2020.06.043.
- Riegler G, Pivec C, Jengojan S, Mayer JA, Schellen C, Trattng S, Bodner G. Cutaneous nerve fields of the anteromedial lower limb – Determination with selective ultrasound-guided nerve blockade. *Clin Anat*. 2021 Jan;34(1):11–18. doi: 10.1002/ca.23582.
- Thallaj A, Marhofer P, Kettner SC, Al-Majed M, Al-Ahaideb A, Moriggl B. High-resolution ultrasound accurately identifies the medial antebrachial cutaneous nerve at the midarm level: a clinical anatomic study. *Reg Anesth Pain Med*. 2011;36(5):499–501. doi: 10.1097/AAP.0b013e318228a359.
- Giannoulis FS, Papoulidis NG, Krexi AV. Lateral antebrachial nerve entrapment. In: Sotereanos DG, Papatheodorou LK, editors. *Compressive Neuropathies of the Upper Extremity* [Internet]. Cham: Springer International Publishing; 2020 [cited 2024 Jun 28]. p. 217–223. Available from: http://link.springer.com/10.1007/978-3-030-37289-7_22
- Meng S, Tinhofner I, Weninger WJ, Grisold W. Anatomical and ultrasound correlation of the superficial branch of the radial nerve. *Muscle Nerve*. 2014 Dec;50(6):939–942. doi: 10.1002/mus.24235.
- Robson AJ, See MS, Ellis H. Applied anatomy of the superficial branch of the radial nerve. *Clin Anat*. 2008 Jan;21(1):38–45. doi: 10.1002/ca.20576.
- Le Corroller T, Bauones S, Acid S, Champsaur P. Anatomical study of the dorsal cutaneous branch of the ulnar nerve using ultrasound. *Eur Radiol*. 2013 Aug 1;23(8):2246–2251. doi: 10.1007/s00330-013-2832-z.
- Matloub HS, Yan JG, Mink Van Der Molen AB, Zhang LL, Sanger JR. The detailed anatomy of the palmar cutaneous nerves and its clinical implications. *J Hand Surg Br*. 1998 Jun;23(3):373–379. doi: 10.1016/s0266-7681(98)80061-2.
- Smith JL, Ebraheim NA. Anatomy of the palmar cutaneous branch of the median nerve: A review. *J Orthop*. 2019 Jun 5;16(6):576–579. doi: 10.1016/j.jor.2019.06.010.
- Tagliafico A, Pugliese F, Bianchi S, Bodner G, Padua L, Rubino M, Martinoli C. High-resolution sonography of the palmar cutaneous branch of the median nerve. *AJR Am J Roentgenol*. 2008 Jul;191(1):107–114. doi: 10.2214/AJR.07.3383.
- Umans H, Kessler J, De La Lama M, Magge K, Liebling R, Negron J. Sonographic assessment of volar digital nerve injury in the context of penetrating trauma. *AJR Am J Roentgenol*. 2010 May;194(5):1310–1313. doi: 10.2214/AJR.09.3884.
- Mitchell CH, Fayad LM, Ahlawat S. Magnetic resonance imaging of the digital nerves of the hand: anatomy and spectrum of pathology. *Curr Probl Diagn Radiol*. 2018 Jan;47(1):42–50. doi: 10.1067/j.cpradiol.2017.02.009.
- Beccioli M, Pivec C, Riegler G. Ultrasound of the lateral femoral cutaneous nerve: a review of the literature and pictorial essay. *J Ultrasound Med*. 2022 May;41(5):1273–1284. doi: 10.1002/jum.15809.
- Fenech M, Roche B, Boyle J. Ultrasound imaging of the femoral and saphenous nerves. *Australas J Ultrasound Med*. 2024 Jul 29;27(4):229–241. doi: 10.1002/ajum.12403.
- Hurdle MF, Weingarten TN, Crisostomo RA, Psimos C, Smith J. Ultrasound-guided blockade of the lateral femoral cutaneous nerve: technical description and review of 10 cases. *Arch Phys Med Rehabil*. 2007 Oct;88(10):1362–1364. doi: 10.1016/j.apmr.2007.07.013.
- Canella C, Demondion X, Guillin R, Boutry N, Peltier J, Cotten A. Anatomic study of the superficial peroneal nerve using sonography. *AJR Am J Roentgenol*. 2009 Jul;193(1):174–179. doi: 10.2214/AJR.08.1898.
- Garrett A, Black AC, Launico MV, Geiger Z. Anatomy, Bony Pelvis and Lower Limb: Superficial Peroneal Nerve (Superficial Fibular Nerve). In: *StatPearls* [Internet]. Treasure Island (FL): StatPearls Publishing; 2025 Jan-. Available from: <http://www.ncbi.nlm.nih.gov/books/NBK534793/>
- Visser LH. High-resolution sonography of the common peroneal nerve: detection of intraneural ganglia. *Neurology*. 2006 Oct 24;67(8):1473–5. doi: 10.1212/01.wnl.0000240070.98910.bc.
- Quinn TJ, Jacobson JA, Craig JG, van Holsbeek MT. Sonography of Morton's neuromas. *AJR Am J Roentgenol*. 2000 Jun;174(6):1723–1728. doi: 10.2214/ajr.174.6.1741723.
- Sharp RJ, Wade CM, Hennessy MS, Saxby TS. The role of MRI and ultrasound imaging in Morton's neuroma and the effect of size of lesion on symptoms. *J Bone Joint Surg Br*. 2003 Sep;85(7):999–1005. doi: 10.1302/0301-620x.85b7.12633.
- Santiago FR, Muñoz PT, Pryest P, Martínez AM, Olleta NP. Role of imaging methods in diagnosis and treatment of Morton's neuroma. *World J Radiol*. 2018 Sep 28;10(9):91–99. doi: 10.4329/wjr.v10.i9.91.